第 35 卷第 11 期
2019 年 11 月

无 机 化 学 学 报
CHINESE JOURNAL OF INORGANIC CHEMISTRY

Vol.35 No.11
2185-2191

# 水热合成具有分级结构的钨酸铋纳米花及其光催化降解四环素性能

张宇晴[1] 曾雪玉[1] 于 凯[1,2] 刘桂芳[1] 曹海雷[1] 吕 健*[,1,2] 曹 荣*[,2]

([1]福建农林大学资源与环境学院福建省土壤环境健康与调控重点实验室,福州 350002)

([2]中国科学院福建物质结构研究所结构化学国家重点实验室,福州 350002)

**摘要**:采用一种简单的无模板水热合成法制备了具有分级结构的钨酸铋纳米花,并将钨酸铋纳米花材料应用于可见光催化去除水中的四环素类抗生素。通过 X 射线粉末衍射、扫描电镜、透射电镜、紫外固体漫反射、比表面分析等一系列物理表征对光催化剂和催化反应体系进行了表征。研究结果表明钨酸铋纳米光催化剂对四环素类抗生素(四环素和土霉素)均具有良好的降解能力。此外,催化剂对碱性溶液中四环素的降解效率普遍较高,且该催化剂表现出良好的循环稳定性。

**关键词**:钨酸铋;纳米花;光催化剂;抗生素

**中图分类号**:O614.61+3;O614.53+2 **文献标识码**:A **文章编号**:1001-4861(2019)11-2191-07

**DOI**:10.11862/CJIC.2019.243

# Hydrothermal Synthesis of Hierarchically Structured Flower-like Bismuth Tungstate for Photocatalytic Tetracycline Degradation

ZHANG Yu-Qing[1] ZENG Xue-Yu[1] YU Kai[1,2] LIU Gui-Fang[1]

CAO Hai-Lei[1] LÜ Jian*[,1,2] CAO Rong*[,2]

([1]*Fujian Provincial Key Laboratory of Soil Environmental Health and Regulation, College of Resources and Environment, Fujian Agriculture and Forestry University, Fuzhou* 350002, *China*)

([2]*State Key Laboratory of Structural Chemistry, Fujian Institute of Research on the Structure of Matter, Chinese Academy of Sciences, Fuzhou* 350002, *China*)

**Abstract:** Hierarchically structured flower-like $Bi_2WO_6$ was fabricated via a simple template-free hydrothermal method. The as-prepared $Bi_2WO_6$ was applied in the removal of tetracycline antibiotics presented in aqueous phases under visible irradiation. The photocatalyst were characterized by a series of physical characterizations including powder X-ray diffraction, scanning electron microscopy, transmission electron microscopy, UV-Vis diffuse reflectance spectra , nitrogen adsorption desorption test etc. The $Bi_2WO_6$ photocatalysts showed excellent degradation capacity towards tetracycline antibiotics (tetracycline (TC) and oxytetracycline (OTC)). Moreover, the TC degradation rates were generally higher in relatively alkaline solutions. The $Bi_2WO_6$ photocatalysts exhibited excellent stability and could be recycled for reuse.

**Keywords:** bismuth tungstate; flower-like; photocatalyst; antibiotic

收稿日期:2019-09-25。收修改稿日期:2019-10-07。

福建农林大学国际合作与交流项目(No.KXGH17010)、中国科学院福建物质结构研究所结构化学国家重点实验室开放基金(No.20170032)和福建省高等学校新世纪优秀人才支持计划资助项目。

*通信联系人。E-mail:jian_lu_fafu@163.com,rcao@fjirsm.ac.cn

## 0 Introduction

Pharmaceutical antibiotics and relative derivatives are emerging pollutants of public concerns originated from pharmaceuticals and personal care products (PPCPs)[1-2]. Since most pharmaceutical antibiotics are poorly metabolized and absorbable, their exposures can cause potential adverse effects on aquatic ecology as well as on human health[3-4]. To solve the environmental issues caused by pharmaceutical antibiotics[5], the development of photocatalysts for antibiotics removal has been considered as one of the most viable advanced oxidation technologies[6-7], in view of the usage of clean and sustainable solar energy[8].

Recently, semiconductor photocatalysts have attracted considerable research focuses due to their excellent capacities in the degradation of organic contaminants[9-11]. Metal oxides and sulfides, such as titanium oxides[12-13], zinc oxides and sulfides[14-16], and cadmium sulfides[17-18], have been widely explored for the photocatalytic degradation of organic compounds. More recently, bismuth tungstates have been demonstrated to show superior performances in the visible-light-driven photocatalysis, thanks to their appropriate band energy, for applications such as water splitting and environmental remediation[19-21]. In this context, various synthetic methods[22-24] have been developed for the fabrication of crystalline $Bi_2WO_6$. However, surface morphology and phase structure of bismuth tungstates are somehow not easily manipulated due to the general application of high temperature reactions. Further to the precise determination on photocatalytic performances, $Bi_2WO_6$ materials prepared at viable and comparable synthetic conditions, with well-defined physical structures and properties, are extremely demanded.

The hydrothermal process has been known as a robust and flexible pathway in the synthesis of advanced materials with high purity, uniform particle size, and excellent dispersion[25]. In this work, hierarchically structured flower-like bismuth tungstate (f-$Bi_2WO_6$) were fabricated through a template-free hydrothermal synthesis. The as-prepared f-$Bi_2WO_6$ was applied for the degradation of tetracycline antibiotics (tetracycline (TC) and oxytetracycline (OTC)) under visible irradiation. Specifically, the f-$Bi_2WO_6$ exhibited photocatalytic degradation efficiency of *ca.* 89.7% (for TC) and *ca.* 75.8% (for OTC), respectively. Furthermore, the f-$Bi_2WO_6$ photocatalyst showed excellent stability at various pH values and could be recycled for reuse, which was promising for the potential application in wastewater treatment.

## 1 Experimental

### 1.1 Materials

$Bi(NO_3)_3\cdot 5H_2O$, $Na_2WO_4\cdot 2H_2O$, ethanol, ethylene glycol, tetracycline, oxytetracycline, *tert*-butyl alcohol, ammonium oxalate and *p*-benzoquinone were commercially purchased and used without further purification. Reaction solutions and stock solutions were prepared using deionized water supplied with a UPT-I-5T ultrapure water system.

### 1.2 Methods

Scanning electron microscopy (SEM) images were photographed by using a JSM6700-F with a working voltage of 10 kV. Transmission electron microscopy (TEM) and high resolution TEM (HRTEM) images were recorded by using an FEIT 20 working at 200 kV. Powder X-ray diffraction (PXRD) was carried out on a Rigaku Miniflex 600 diffractometer with Cu $K\alpha$ radiation ($\lambda$=0.154 nm, $U$=40 kV, $I$=40 mA, $2\theta$=10°~80°). $N_2$ adsorption-desorption isotherms were obtained on a Micromeritics ASAP 2460 instrument and used for Brunauer-Emmett-Teller (BET) surface area and pore size distribution (PSD) calculations. UV-Vis and diffuse reflectance spectra (DRS) were recorded on a Shimadzu UV-Vis spectrophotometer (UV-2550).

### 1.3 Synthesis

$Bi(NO_3)_3\cdot 5H_2O$ (2.0 mmol) and $Na_2WO_4\cdot 2H_2O$ (1.0 mmol) were dissolved in 30 mL mixed ethylene glycol and ethanol (1:2, *V*/*V*), followed by stirring for 30 min at 500 $r\cdot min^{-1}$ and sealed in a solvothermal autoclave and kept in an oven (160 ℃) for 12 h. The f-$Bi_2WO_6$ was isolated as white powder product and washed with ultrapure water and absolute ethanol, respectively, and collected by using a centrifuge and dried overnight in

an oven (50 ℃).

### 1.4 Photocatalytic reaction

In a typical procedure, the f-$Bi_2WO_6$ photocatalyst (20 mg) and tetracycline solution (100 mL, 20 $mg\cdot L^{-1}$) were added in a Pyrex glass vessel (200 mL) with simultaneous shaking. The above mixture was left for 30 min in dark then exposed to visible light. Photocatalytic experiments were monitored by UV-Vis measurements of the characteristic absorbency of tetracycline molecules after certain time intervals.

Degradation efficiency was estimated by the following equation: $D=C/C_0\times100\%$, where $D$ is the degradation efficiency, and $C_0$ and $C$ is the initial and tested characteristic absorbencies of tetracycline, respectively. The rate constant ($k$) was estimated by the following equation: $-\ln(C/C_0)=kt$.

### 1.5 Photocatalyst stability test

Stability of the f-$Bi_2WO_6$ photocatalyst was studied by repeated cycles of photocatalytic reactions under set conditions. Between two consecutive runs of a cycling reaction, the photocatalyst was recycled by using a centrifuge and washed with ultrapure water and ethanol for several times and dried at 50 ℃ in an oven. The f-$Bi_2WO_6$ was then separated at the end of a cycling reaction, washed, and dried as stated above and used for further PXRD measurements.

## 2 Results and discussion

### 2.1 Physical characterization

Surface morphology of the f-$Bi_2WO_6$ was revealed by using SEM and TEM techniques. As shown in Fig. 1a and 1b, the f-$Bi_2WO_6$ displayed hierarchically flower-like structure (around 1.0 micron in size and *ca.* 20 nm in thickness) assembled from plates of bismuth tungstates. TEM images also clearly showed the flower-like structure (Fig.1c) and lattice fringes with *d*-spacing of *ca.* 0.312 nm (Fig.1d), which corresponded to the (113) crystal plane of f-$Bi_2WO_6$. PXRD was applied to identify the phase purity of f-$Bi_2WO_6$ (Fig.2a). The characteristics at 28.31°, 32.93°, 47.28°, 55.83°, 58.56°, 68.75°, 75.96 and 78.03° were well indexed as (113), (020), (028), (313), (226), (400), (139) and (145) crystal planes of orthorhombic $Bi_2WO_6$ (Fig.2a; PDF No.73-1126)[26]. $N_2$ adsorption/desorption isotherms were recorded to evaluate the porosity of the f-$Bi_2WO_6$. As shown in Fig.2b, the f-$Bi_2WO_6$ showed typical adsorption/desorption isotherms for nanomaterials with clear hysteresis loop,

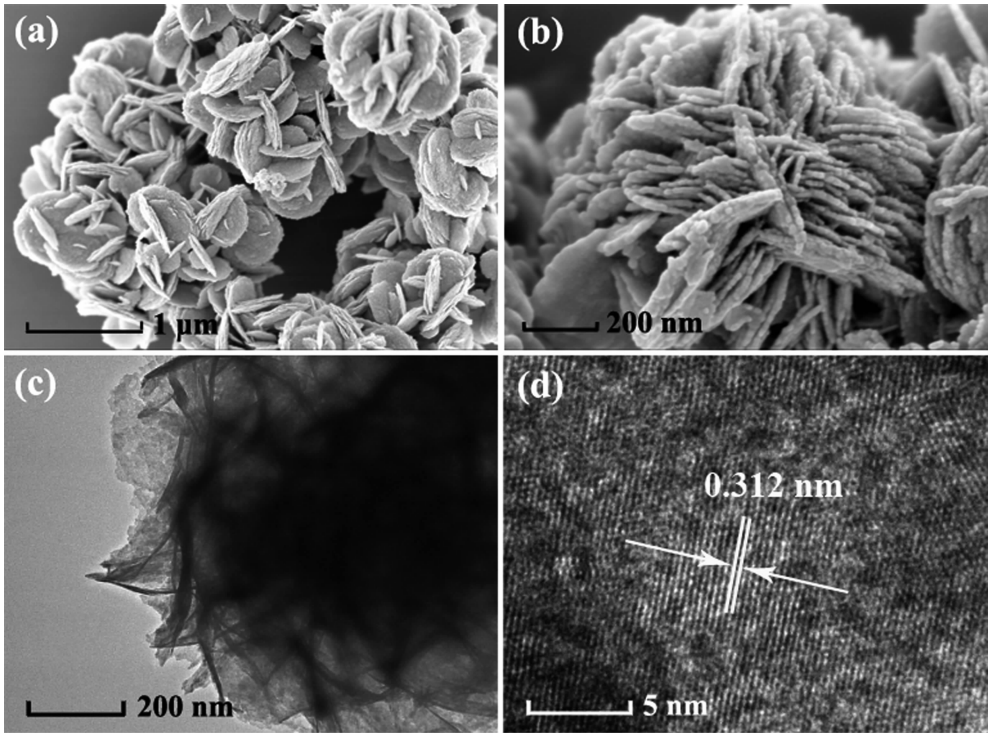


Fig.1　SEM (a, b) and TEM (c, d) images of the f-$Bi_2WO_6$

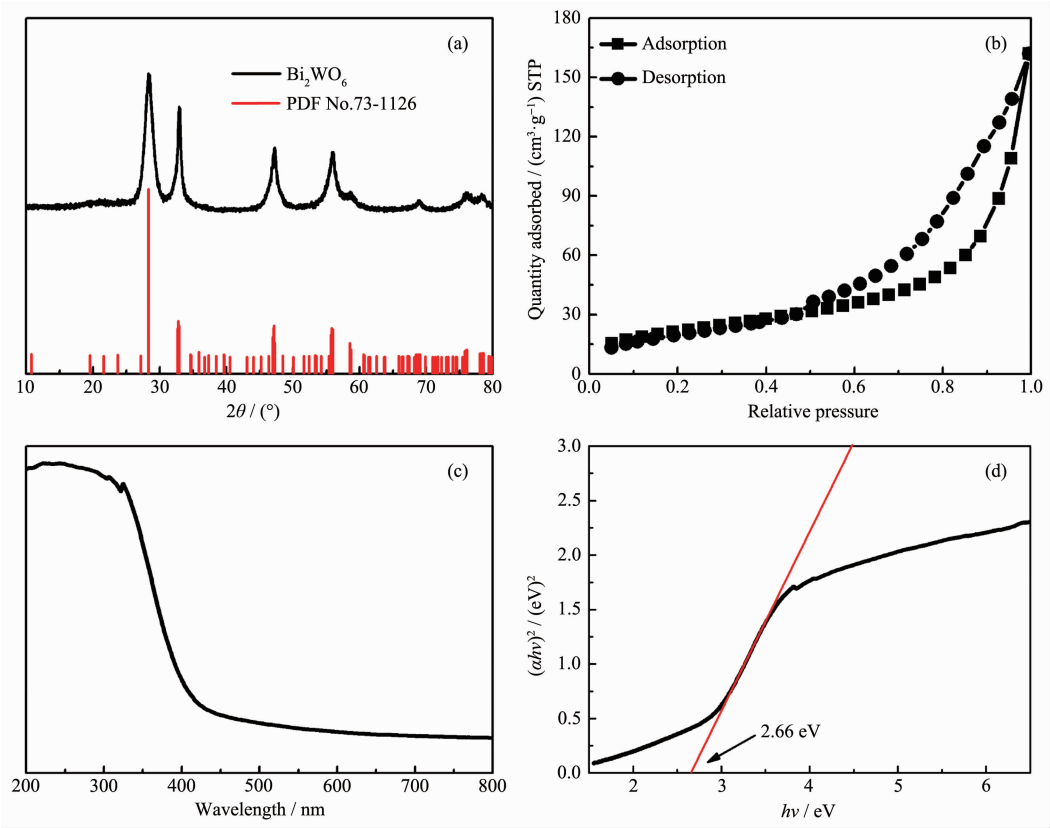


Fig.2 (a) PXRD patterns, (b) $N_2$ adsorption-desorption isotherms, (c) DRS spectrum, and (d) K-M plot of the f-$Bi_2WO_6$

possessing dominant mesopores. The BET surface area was estimated to be *ca.* 78 $m^2 \cdot g^{-1}$ which was fairly reasonable for hierarchically structured flower-like $Bi_2WO_6$. UV-Vis diffuse reflectance spectra (DRS) of the f-$Bi_2WO_6$ are shown in Fig.2c. The absorption bands in the visible region indicated considerable light harvesting capacity of the f-$Bi_2WO_6$, which generally favored the visible-light-driven photocatalytic activity for target reactions[27]. The main band structure of the f-$Bi_2WO_6$ in the visible region was calculated by the converted Kubelka-Munk (K-M) equation $\alpha h\nu = A(h\nu - E_g)^{1/2}$, where $\alpha$ is the adsorption coefficient, $h\nu$ is the photon energy, $E_g$ is the direct band gap (eV), and $A$ is a constant[28-29]. The calculated $E_g$ for the f-$Bi_2WO_6$ was 2.66 eV (Fig.2d), which was suitable for excitation under visible irradiation.

## 2.2 Photocatalytic activity

Photocatalytic activity of the f-$Bi_2WO_6$ was studied towards the degradation of tetracycline antibiotics (TC and OTC) under visible irradiation. In a typical procedure, photocatalyst was first immersed in TC/OTC solutions and reacted in dark for 30 min to reach the adsorption/desorption equilibrium. Upon visible irradiation, the UV-Vis absorption characteristics of TC/OTC decreased gradually with time, indicating continuous photocatalytic TC/OTC degradation. Of note, the f-$Bi_2WO_6$ was able to degrade *ca.* 75.8% of OTC and *ca.* 89.7% of TC within 1 h (Fig.3a), which was comparable to some of the best performing photocatalysts for the degradation of tetracycline antibiotics documented in the literatures[30]. Quantitatively, the apparent rate constant $k$ of 0.041 9 $min^{-1}$ for TC degradation was calculated by the pseudo-first-order reaction kinetics equation (Fig.3a, inset), which was approximately 2.1 times of that for the cubic $Bi_2MoO_6$ and 4.4 times of that for the $WO_3$/g-$C_3N_4$ Z-scheme photocatalysts showing similar TC degradation efficiencies[31-32]. The excellent photocatalytic capacity of the f-$Bi_2WO_6$ was likely derived from the enhanced separation efficiency of photogenerated charge carriers at host-guest interfaces.

To further investigate the mechanism for TC

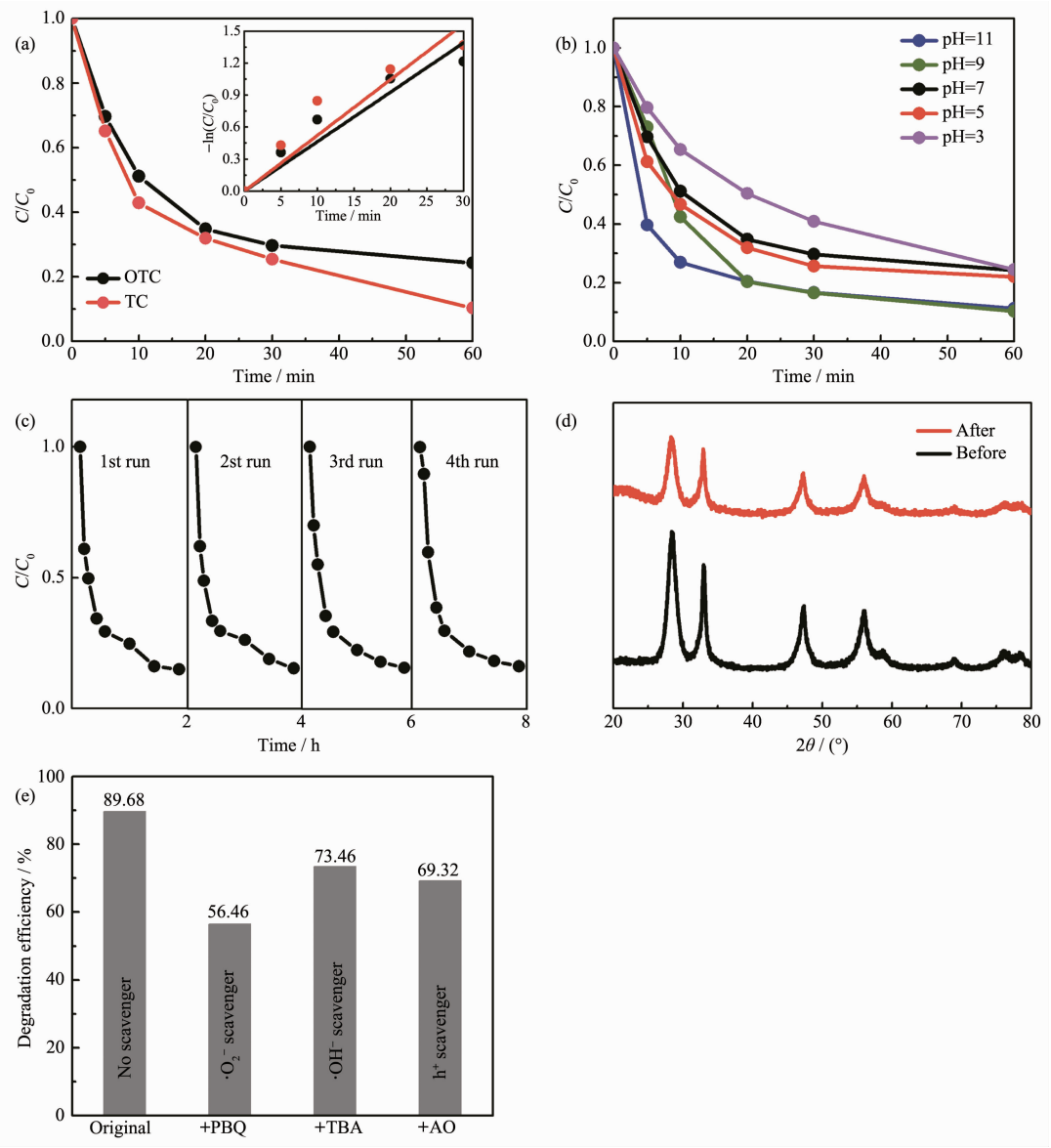


Fig.3　(a) Photocatalytic TC and OTC degradation efficiency of the f-$Bi_2WO_6$; (b) Photocatalytic TC degradation at various pH values; (c) Cyclic TC degradation reactions; (d) PXRD of the f-$Bi_2WO_6$ before and after cyclic reactions; (e) Photocatalytic efficiency of the f-$Bi_2WO_6$ with exposure to various scavengers

degradation, scavenger experiments were applied to detect photogenerated active species[33-34]. Considerable decreases on the photocatalytic efficiency of the f-$Bi_2WO_6$ were observed upon addition of ammonium oxalate (AO), *tert*-butyl alcohol (TBA) and *p*-benzoquione (PBQ), which were used as scavengers for $h^+$, ·OH and $\cdot O_2^-$ radicals, respectively[35]. Specifically, PBQ exhibited better quenching effects towards the photo-catalytic reactions, which was rather superior to AO and TBA. Specifically, $\cdot O_2^-$ accounted for *ca.* 33.2% of the total degradation efficiency, whereas $h^+$ (*ca.* 20.4%) and ·OH (*ca.* 16.2%) contributed relatively less to the overall photodegradation of tetracycline molecules (Fig.3e). These results suggested $\cdot O_2^-$ radicals were likely dominant active species, whereas $h^+$ and ·OH radicals played minor roles in this current system.

We thus propose the visible-light-driven photocatalysis might be initiated by the fast generation and separation of photogenerated carriers ($h^+$, $e^-$), followed by electron transfer from the valence bond (VB) to conduction band (CB) of $Bi_2WO_6$[36]. The highly reduc-

tive $e^-$ takes part in the formation of a series of active species including ·OH and $\cdot O_2^-$ radicals, of which ·OH is initiated via a complex process involving the reduction of $H_2O_2$ generated by $\cdot O_2^-$ species. The oxidative $h^+$, ·OH and $\cdot O_2^-$ attack and degrade organic substrates (TC and OTC) into secondary and final products ($H_2O$ and $CO_2$).

### 2.3 Stability

We further studied photocatalytic TC degradation at various pH values. As shown in Fig.3b, the f-$Bi_2WO_6$ displayed faster and more efficient TC degradation rate at higher pH values (9.0 and 11.0), than the TC degradation rate at lower pH value of 3.0, 5.0 and 7.0. These results indicated photocatalytic TC degradation were favored in alkaline solutions which might be reasonable to carry out TC removal before acidification or appropriate pH adjustment would be necessary during wastewater treatment. Moreover, recycling reactions of TC degradation were performed to verify the photostability and reusability of the f-$Bi_2WO_6$. It was demonstrated that the f-$Bi_2WO_6$ could preserve more than 95% of its initial catalytic ability at the end of four consecutive runs, as indicated in Fig.3c. PXRD patterns recorded on the f-$Bi_2WO_6$ before and after recycling reactions matched well with each other (Fig.3d), suggesting significant structural and crystalline stability of the photocatalyst. These results suggested that the as-prepared f-$Bi_2WO_6$ was promising for the potential application in wastewater treatment.

## 3 Conclusions

In summary, we proposed a facile hydrothermal synthetic pathway to prepare hierarchically structured flower-like bismuth tungstate. The as-prepared f-$Bi_2WO_6$ photocatalysts exhibited considerably superior photocatalytic capacity towards tetracycline degradation at various pH, as well as cyclic photocatalytic reactions. Active species such as $h^+$, ·OH and $\cdot O_2^-$ were believed to be keys that were responsible for the high photocatalytic efficiency of the materials. Further study to fabricate $Bi_2WO_6$ photocatalysts with different morphology in similar reaction systems is currently underway, which may help to determine the specific role of structural morphology and possible effects of structure control on the optimization of photocatalytic activity of bismuth tungstate.

**Acknowledgements:** We thank the International Science and Technology Cooperation and Exchange Project of Fujian Agriculture and Forestry University (Grant No.KXGH17010), the State Key Laboratory of Structural Chemistry (Grant No. 20170032) and the New Century Excellent Talents in Fujian Province University for funding.

## References:

[1] Sarmah A K, Meyer M T, Boxall A B A. *Chemosphere*, **2006**, **65**:725-759

[2] Martinez J L. *Environ. Pollut.*, **2009**,**157**:2893-2902

[3] Pomati F, Castiglioni S, Zuccato E, et al. *Environ. Sci. Technol.*, **2006**,**40**:2442-2447

[4] Yang L H, Ying G G, Su H C, et al. *Environ. Toxicol. Chem.*, **2008**,**27**:1201-1208

[5] Kim S, Eichhorn P, Jensen J N, et al. *Environ. Sci. Technol.*, **2005**,**39**:5816-5823

[6] Yu H J, Shi R, Zhao Y F, et al. *Adv. Mater.*, **2016**,**28**:9454-9477

[7] Tian Y, Hua G, Xu W, et al. *J. Alloys Compd.*, **2011**,**509**: 724-730

[8] Li S H, Liu S, Colmenares J C, et al. *Green Chem.*, **2016**,**18**: 594-607

[9] He X, Nguyen V, Jiang Z, et al. *Catal. Sci. Technol.*, **2018**, **8**:2117-2123

[10]Huang H B, Wang Y, Cai F Y, et al. *Front. Chem.*, **2017**,**5**: 123

[11]WANG Xiao-Li(王晓丽), ZHANG Lin-Ping(张琳萍), ZHOU Pei-Wen(周培文), et al. *Chinese J. Inorg. Chem.*(无机化学学报), **2019**,**35**(5):812-818

[12]Calza P, Medana C, Pazzi M, et al. *Appl. Catal. B*, **2004**,**53**: 63-69

[13]Baran W, Adamek E, Sobczak A, et al. *Appl. Catal. B*, **2009**,**90**:516-525

[14]Xue X Y, Zang W L, Deng P, et al. *Nano Energy*, **2015**,**13**: 414-422

[15]da Silva G T S T, Carvalho K T G, Lopes O F, et al. *ChemCatChem*, **2017**,**9**:3795-3804

[16]Hu J S, Ren L L, Guo Y G, et al. *Angew. Chem. Int. Ed.*, **2005**,**44**:1269-1273

[17]Huang H B, Wang Y, Jiao W B, et al. *ACS Sustain. Chem.*

*Eng.*, **2018**,**6**:7871-7879

[18]Cao H L, Cai F Y, Yu K, et al. *ACS Sustain. Chem. Eng.*, **2019**,**7**:10847-10854

[19]Li G, Zhang D, Yu J C, et al. *Environ. Sci. Technol.*, **2010**, **44**:4276-4281

[20]CUI Yu-Min(崔玉民), HONG Wen-Shan(洪文珊), LI Hui-Quan(李慧泉), et al. *Chinese J. Inorg. Chem.*(无机化学学报), **2014**,**30**(2):431-441

[21]Li S Z, Yang Y S, Liu L J, et al. *Chem. Eng. J.*, **2018**,**334**: 1691-1698

[22]Kim N, Vannier R N, Grey C P. *Chem. Mater.*, **2005**,**17**: 1952-1958

[23]Zhao Q, Liu L J, Li S Z, et al. *Appl. Surf. Sci.*, **2019**,**465**: 164-171

[24]Cao S W, Shen B J, Tong T, et al. *Adv. Funct. Mater.*, **2018**, **28**:1800136

[25]SONG Qiang(宋强), LI Li(李莉), LUO Hong-Xiang(罗鸿祥), et al. *Chinese J. Inorg. Chem.*(无机化学学报), **2017**,**33**(7): 1161-1171

[26]Guo S, Li X F, Wang H Q, et al. *J. Colloid Interface Sci.*, **2012**,**369**:373-380

[27]Xu Y, Zhang W D. *Eur. J. Inorg. Chem.*, **2015**,**2015**:1744-1751

[28]Yu J G, Yu Y F, Zhou P, et al. *Appl. Catal. B*, **2014**,**156**: 184-191

[29]Wang S, Guan B Y, Lou X W D. *J. Am. Chem. Soc.*, **2018**, **140**:5037-5040

[30]Chen M J, Chu W. *Chem. Eng. J.*, **2016**,**296**:310-318

[31]Xiao T T, Tang Z, Yang Y, et al. *Appl. Catal. B*, **2018**,**220**: 417-428

[32]Xiong J Y, Cheng G, Li G F, et al. *RSC Adv.*, **2011**,**1**:1542-1553

[33]Wang P, Xian J, Chen J, et al. *Appl. Catal. B*, **2014**,**144**: 644-653

[34]Hou Y, Yang J, Lei C J, et al. *ACS Sustainable Chem. Eng.*, **2018**,**6**:6497-6506

[35]Wang J, Wang P, Cao Y, et al. *Appl. Catal. B*, **2013**,**136**:94-102

[36]Bera R, Kundu S, Patra A. *ACS Appl. Mater. Interfaces*, **2015**,**7**:13251-13259